

Control of multistability through local sensitivity analysis: application to cellular decision-making networks

Rodrigo Moreno-Morton^{†1} and Alessio Franci^{†2}

Abstract—Control of multistable dynamics has important applications, from physics to biology but the complexity of the systems of differential equations used for their modeling often makes this problem intractable from a global perspective. Here, we propose that for a certain class of multi-stable dynamical systems, including monotone systems, linearized control at the stable and saddle points of the multi-stable dynamics can lead to predictable global changes in the relative sizes and depths of its basins of attraction. Our parameter control signal is computationally cheap and provides counter-intuitive information about the sensitive parameters to be manipulated in an experimental setting.

I. INTRODUCTION

Multistable dynamics and their control appear in a variety of physical, engineered, and biological systems [1]. Opinion-formation and decision-making networks also exhibit multistability and are receiving increasing attention due to their relevance in sociopolitical systems and for collective behaviors in both biological and artificial agent groups. In these networks, each attractor corresponds to a decision state (see [2] and references therein). Another important example of multistable decision-making are molecular regulatory networks, where decisions correspond to cellular phenotypes [3]. Cellular decision-making can be functional, e.g., development, but also deleterious for the organism, e.g., tumor formation.

A well studied case of cellular decision-making with both functional or deleterious consequences is the epithelial-mesenchymal transition (EMT), a change in phenotype of epithelial cells from a clearly polarized, epithelium-adhered cell (epithelial phenotype) to a non-polarized, free-moving cell (mesenchymal phenotype) [4], [5]. EMT plays an important role in several stages of embryonic development and tissue repair but also in tumor metastasis [6]. Understanding how the EMT is regulated and how it may be controlled is relevant both for biology and medicine.

Global analysis and control of multi-stable dynamics are hard in general. Although almost global Lyapunov functions are known to exist for multistable systems [7], their analytical computation is impossible except for simple low-dimensional examples. Some local approaches, based on the model linearization, have been developed for discrete-time dynamical systems with chaotic dynamics [1].

Motivated by EMT control, in this paper we focus on multistable dynamics in which the only attractors are exponentially stable equilibria and in which the boundaries of the basins

of attraction are the stable manifolds of saddle points. Monotone dynamical systems [8] in any dimension are important representatives of this class of systems.

The paper contributions are the following. Under suitable monotonicity assumptions, we prove the existence of a simple relation between the stability margin of an equilibrium of a one-dimensional multistable dynamical system and the size of its basin of attraction. We single out a class of multistable dynamical systems in arbitrary dimension for which the one-dimensional theory suggests a simple strategy to control the relative size and depth of the various basins of attraction. Although grounded on heuristic arguments, our control strategy solely uses the local sensitivity of the linearized model dynamics at the relevant equilibria. In particular, it does not require the knowledge of an analytic expression for the model almost-global Lyapunov function. Its effectiveness is illustrated on a simple two-dimensional monotone dynamical system and on a novel four-dimensional model of the EMT.

The one-dimensional theory is illustrated in Section III. The relevant class of high-dimensional dynamics and the proposed strategy for their multistability control are introduced in Section IV. Applications to a two-dimensional monotone dynamics and to a four-dimensional EMT model are illustrated in Section IV-G and Section V. Limitations are discussed in Section VI. Section VII provides the project GitHub page.

II. NOTATION AND DEFINITIONS

\mathbb{R} denotes the set of real numbers. \mathbb{N} denotes the set of positive integers. \mathbb{C} denotes the set of complex numbers. $\langle \cdot, \cdot \rangle : \mathbb{R}^n \times \mathbb{R}^n \rightarrow \mathbb{R}$ denotes the Euclidean product in \mathbb{R}^n and $\|\cdot\| : \mathbb{R}^n \rightarrow \mathbb{R}$ its induced norm. Given $x \in \mathbb{R}$, $\text{sgn}(x)$ denotes its sign, i.e., $\text{sgn}(x) = -1$ if $x < 0$, $\text{sgn}(x) = 0$ if $x = 0$, and $\text{sgn}(x) = 1$ if $x > 0$. Given $z \in \mathbb{C}$, $\text{Re}(z)$ denotes its real part. A set $\mathcal{K} \subset \mathbb{R}^n$ is a linear cone if for all $x \in \mathcal{K}$ and all $a > 0$, $ax \in \mathcal{K}$. An orthant $K \subset \mathbb{R}^n$ is the cone $\{x \in \mathbb{R}^n : (-1)^{m_i} x_i \geq 0, i = 1, \dots, n, m_i \in \{0, 1\}\}$.

Consider a smooth dynamical system

$$\frac{dx}{dt} =: \dot{x} = f(x), \quad f : \mathbb{R}^n \rightarrow \mathbb{R}^n. \quad (1)$$

with flow $\varphi : \mathbb{R}^n \times \mathbb{R} \rightarrow \mathbb{R}^n$, i.e., given $y \in \mathbb{R}^n$, $x(t) = \varphi(y, t)$ is the solution of (1) at time t with initial conditions $x(0) = y$. An equilibrium x^* of (1) is called hyperbolic if the Jacobian $\frac{\partial f}{\partial x}(x^*) \in \mathbb{R}^{n \times n}$ has no eigenvalues on the imaginary axis. The stable manifold of an equilibrium x^* is the set $\{x \in \mathbb{R}^n : \lim_{t \rightarrow \infty} \varphi(x, t) = x^*\}$. The unstable manifold of an equilibrium x^* is the set $\{x \in \mathbb{R}^n : \lim_{t \rightarrow -\infty} \varphi(x, t) = x^*\}$. If a hyperbolic equilibrium x^* is stable, that is, if $\frac{\partial f}{\partial x}(x^*)$ has only eigenvalues with negative real part, then its stable manifold is called its

This work was supported by DGAPA-PAPIIT(UNAM) grant n. IN102420 and Conacyt CB grant n. A1-S-10610.

[†] Math Department at the Faculty of Sciences, National Autonomous University of Mexico (UNAM). ¹luimormor@gmail.com. ²afranci@ciencias.unam.mx

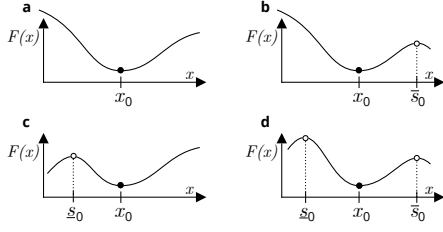


Fig. 1: Unbounded vs bounded one-dimensional basins of attraction. **a.** Unbounded. **b,c.** Half-bounded. **d.** Bounded. Stable equilibria are denoted by dots; unstable equilibria by circles.

basin of attraction. A set $U \subset \mathbb{R}^n$ is called invariant for model (1) if $x \in U$ implies $\varphi(x, t) \in U$ for all $t \in \mathbb{R}$. A trajectory is called heteroclinic if $\lim_{t \rightarrow -\infty} \varphi(x, t) = x_1^*$ and $\lim_{t \rightarrow \infty} \varphi(x, t) = x_2^*$ for two distinct equilibria x_1^*, x_2^* . Given a linear cone \mathcal{K} , a trajectory $\varphi(x, t)$ is called \mathcal{K} -monotone if $\varphi(x, t_2) - \varphi(x, t_1) \in \mathcal{K}$ for all $t_2 > t_1$.

III. ONE-DIMENSIONAL THEORY

Consider a one-dimensional dynamical system

$$\dot{x} = f(x) = -F'(x) \quad (2)$$

where $f : \mathbb{R} \rightarrow \mathbb{R}$ is smooth and F is a primitive of $-f$, i.e., $F(x) = -\int_0^x f(y)dy + C$, $C \in \mathbb{R}$. $F(x)$ is an almost global Lyapunov function for (2), in the sense of [7]. Suppose that x_0 is an exponentially stable equilibrium of (2), i.e.,

$$F'(x_0) = 0, \quad F''(x_0) > 0. \quad (3)$$

Generically there are three possible cases for the geometry of the basin of attraction of x_0 : unbounded (Figure 1a), half-bounded (Figure 1b,c), bounded (Figure 1d). Boundaries of the basin of attraction, when they exist, are given by unstable points $\underline{s}_0, \bar{s}_0$, with $\underline{s}_0 < x_0 < \bar{s}_0$, satisfying¹

$$F'(\underline{s}_0) = F'(\bar{s}_0) = 0, \quad F''(\underline{s}_0), F''(\bar{s}_0) < 0. \quad (4)$$

We focus on the bounded case (Figure 1d) but we also remark that our theoretical developments apply naturally to the bounded side of the half-bounded cases (Figure 1b,c).

Our goal is understanding how the presence of possible control parameters in model (2) affect the depth (i.e., local stability) and size of the basin of attraction of x_0 , as well as understanding how depth and size can be related.

A. Increasing local stability margins of x_0 increases the global size of its basin of attraction

Suppose a parameter α tunes the stability of x_0 as

$$\dot{x} = -F'(x) - \kappa(x, \alpha), \quad (5)$$

where $\kappa : \mathbb{R} \times \mathbb{R} \rightarrow \mathbb{R}$ is smooth and satisfies the following *monotonicity conditions*

$$\begin{aligned} \kappa(x, 0) &= 0, \quad \text{sgn} \left(\frac{\partial \kappa}{\partial x}(x, \alpha) \right) = \text{sgn}(\alpha), \\ \text{sgn} \left(\frac{\partial \kappa}{\partial \alpha}(x, 0) \right) &= \text{sgn}(x - x_0). \end{aligned} \quad (6)$$

¹We denote the unstable equilibria with an s because in higher dimension they will correspond to *saddle* points.

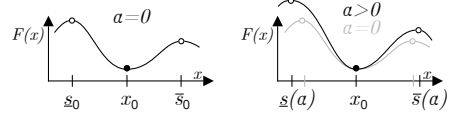


Fig. 2: Increasing the stability of an exponentially stable equilibrium increases the size of its basin of attraction, and vice-versa.

As representative examples, $\kappa(x, \alpha) = \alpha(x - x_0)$ or $\kappa(x, \alpha) = \alpha \bar{\kappa}(x)$ with $\bar{\kappa}(\cdot)$ strictly monotone increasing and $\bar{\kappa}(x_0) = 0$. Observe that model (5) has almost global Lyapunov function $V(x, \alpha) = F(x) + \int_0^x \kappa(y, \alpha)dy$.

Increasing α increases the stability margins of x_0 because $\frac{\partial}{\partial \alpha} \frac{\partial \dot{x}}{\partial x} \Big|_{x=x_0} < 0$, which implies $\frac{\partial \dot{x}}{\partial x} \Big|_{x=x_0} < \frac{\partial \dot{x}}{\partial x} \Big|_{x=x_0} < 0$, i.e., the eigenvalue of the linearization at x_0 becomes more negative as α is increased.

Let $\underline{s}(\alpha)$ and $\bar{s}(\alpha)$ be the boundaries of the basin of attraction of x_0 for sufficiently small α . In particular, $\underline{s}(0) = \underline{s}_0$ and $\bar{s}(0) = \bar{s}_0$.

Lemma III.1. *The two functions $\underline{s}(\alpha)$ and $\bar{s}(\alpha)$ are differentiable at $\alpha = 0$. Furthermore $\underline{s}'(0) < 0$ and $\bar{s}'(0) > 0$.*

Proof. By definition $V'(\underline{s}(\alpha), \alpha) \equiv 0$ for α sufficiently small. Differentiating with respect to α we get

$$\left(F''(\underline{s}(\alpha)) + \frac{\partial \kappa}{\partial x}(\underline{s}(\alpha), \alpha) \right) \underline{s}'(\alpha) + \frac{\partial \kappa}{\partial \alpha}(\underline{s}(\alpha), \alpha) = 0. \quad (7)$$

Invoking (4) and (6), it follows that $\underline{s}'(0) = -\frac{\partial \kappa}{\partial \alpha}(\underline{s}_0, 0)/F''(\underline{s}_0) < 0$. Similarly, we get $\bar{s}'(0) > 0$. ■

The following theorem, illustrated in Figure 2, is a direct corollary of Lemma III.1.

Theorem III.1. *In model (5)-(6), enhancing the stability of x_0 , that is, making $\frac{\partial \dot{x}}{\partial x} \Big|_{x=x_0}$ more negative, by increasing α , also increases the size of its basin of attraction.*

Under suitable assumptions, a simple converse theorem can also be proved, i.e., increasing the size of the basin of attraction of x_0 increases its stability margins. Its statement and proof are not included due to space constraints.

IV. HIGH-DIMENSIONAL GENERALIZATION

Our goal is to apply the results of the one-dimensional theory in Section III to higher-dimensional systems of the form

$$\dot{x} = F(x, \pi), \quad (8)$$

where $x \in \mathbb{R}^n$, $\pi \in \mathbb{R}^m$ is a vector of parameters, and $F : \mathbb{R}^n \times \mathbb{R}^m \rightarrow \mathbb{R}^n$ is smooth.

Definition IV.1. An unstable equilibrium of model (8) is called a *saddle point* if its stable manifold is $n-1$ -dimensional and an *unstable equilibrium* otherwise.

Assumption IV.1. For all x_0 , the trajectory $\varphi(x_0, t)$ of (8) is bounded and the only attractors of (8) are exponentially stable equilibria with real simple eigenvalues. The basins of attraction are separated by the union of the stable manifolds of saddle points and any heteroclinic trajectory from a saddle to a stable equilibrium is K -monotone for some orthant K .

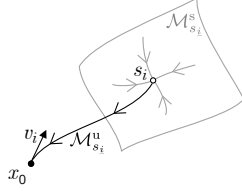


Fig. 3: The one-dimensional invariant dynamics over the K -monotone heteroclinic trajectory $\mathcal{M}_{s_i}^u$ between a stable point x_0 and a saddle point s_i , and associated eigenvector v_i at x_0 .

Evidently, Assumption IV.1 is satisfied by one-dimensional dynamical systems. Another important class of dynamics satisfying this assumption are monotone dynamical systems with bounded trajectories [8, Theorem 2.6 and below].

Under Assumption IV.1, each stable equilibrium $x_0 \in \mathbb{R}^n$ of model (8) is surrounded by a set of saddle points $s_1, \dots, s_l \in \mathbb{R}^n$, $l \leq n$, and associated stable and unstable manifolds, $\mathcal{M}_{s_i}^s$ and $\mathcal{M}_{s_i}^u$, $i = 1, \dots, l$, respectively. The union $\bigcup_{i=1}^l \mathcal{M}_{s_i}^s$ of the saddle stable manifolds defines the boundary of the basin of attraction of x_0 . Each saddle unstable manifold $\mathcal{M}_{s_i}^u$ is the monotone heteroclinic trajectory connecting x_0 and s_i (see Figure 3). Let

$$J_x^\pi = \frac{\partial F}{\partial x}(x, \pi) \quad (9)$$

be the Jacobian of model (8) at x with parameters π . Then each $\mathcal{M}_{s_i}^u$ is tangent at x_0 to a distinct eigenvector v_i of $J_{x_0}^\pi$ with associated eigenvalue $\lambda_i < 0$.

A. A heuristic argument.

To generalize the one-dimensional theory to model (8) we rely on the following argument.

- i) Multistability in (8) is organized by the saddle stable manifolds $\mathcal{M}_{s_i}^s$ and the saddle-to-stable equilibrium heteroclinic orbits (unstable manifolds) $\mathcal{M}_{s_i}^u$.
- ii) Because dynamics on the one-dimensional invariant sets $\mathcal{M}_{s_i}^u$ are monotone, the one-dimensional theory, in particular condition (6), approximately applies along each $\mathcal{M}_{s_i}^u$. This ensures that pushing the saddle s_i (and therefore its stable manifold $\mathcal{M}_{s_i}^s$) away from a stable equilibrium x_0 and decreasing the eigenvalue λ_i of $J_{x_0}^\pi$ associated to v_i (as in Figure 3) are two complementary ways of enlarging the basin of attraction of x_0 .

In light of this argument, the proposed generalization involves two control strategies: eigenvalue control and saddle location control. We introduce them in the following sections.

B. Two useful lemmas

The following basic lemmas provide the basic tools for eigenvalue and saddle location control.

Lemma IV.1. *Let x^* be a hyperbolic equilibrium of (8), i.e., $F(x^*, \pi) = 0$. Then $\frac{\partial x^*}{\partial \pi_i} = -(J_{x^*}^\pi)^{-1} \frac{\partial F}{\partial \pi_i}(x^*, \pi)$.*

Proof. Because x^* is hyperbolic, $J_{x^*}^\pi$ is not singular and the lemma follows by the implicit function theorem. ■

Lemma IV.2. *Let x^* be a hyperbolic equilibrium of (8). Let $\lambda \in \mathbb{C}$ be an eigenvalue of $J_{x^*}^\pi$ with left eigenvector $w \in \mathbb{C}^n$ and right eigenvector $v \in \mathbb{C}^n$. The total derivative $D_i \lambda = \frac{\partial \lambda}{\partial x} \frac{\partial x^*}{\partial \pi_i} + \frac{\partial \lambda}{\partial \pi_i}$ of λ with respect to π_i is given by $D_i \lambda = \frac{w^T D_i J_{x^*}^\pi v}{w^T v}$, where $D_i J_{x^*}^\pi$ is the total derivative of $J_{x^*}^\pi$ with respect to π_i , i.e. $D_i J_{x^*}^\pi = \frac{\partial J_{x^*}^\pi}{\partial x} \frac{\partial x^*}{\partial \pi_i} + \frac{\partial J_{x^*}^\pi}{\partial \pi_i}$.*

Proof. By differentiating the equality $w^T J_{x^*}^\pi v = w^T \lambda v$ with respect to π_i and noticing that the terms involving derivatives of w^T and v cancel out, we obtain $w^T \left(\frac{\partial J_{x^*}^\pi}{\partial x} \frac{\partial x^*}{\partial \pi_i} + \frac{\partial J_{x^*}^\pi}{\partial \pi_i} \right) v = w^T \left(\frac{\partial \lambda}{\partial x} \frac{\partial x^*}{\partial \pi_i} + \frac{\partial \lambda}{\partial \pi_i} \right) v$ and the result follows. ■

C. Eigenvalue control by local sensitivity analysis

Consider a stable equilibrium x_0 of model (8) with parameters π and let Assumption IV.1 hold. Let $\lambda < 0$ be an eigenvalue of $J_{x_0}^\pi$ with left eigenvector $w \in \mathbb{R}^n$ and right eigenvector $v \in \mathbb{R}^n$. Our goal is to make λ more negative through suitable parameter variation. The gradient of λ with respect to the vector of parameters can be computed using Lemma IV.2 as $\nabla \lambda = [D_1 \lambda, \dots, D_m \lambda] = \left[\frac{w^T D_1 J_{x_0}^\pi v}{w^T v}, \dots, \frac{w^T D_m J_{x_0}^\pi v}{w^T v} \right]$, where $D_i J_{x_0}^\pi = \frac{\partial J_{x_0}^\pi}{\partial x} \frac{\partial x_0}{\partial \pi_i} + \frac{\partial J_{x_0}^\pi}{\partial \pi_i}$ and $\frac{\partial x_0}{\partial \pi_i}$ can be computed as in Lemma IV.1. The direction in the parameter space that leads to the fastest decrease of λ is therefore

$$d_\lambda = - \frac{\nabla \lambda}{\|\nabla \lambda\|}. \quad (10)$$

Suppose all parameters can be controlled independently and no other parametric constraints are present. The proposed control strategy to decrease λ by $\delta \lambda > 0$ units is the following, where $0 < \varepsilon \ll 1$ and $n_{\text{ite}} \in \mathbb{N}$ are control hyperparameters.

Control Strategy IV.1. Eigenvalue Control

1. Compute (10) at the current equilibrium and parameter values.
2. Update the parameters: $\pi \leftarrow \pi + \varepsilon d_\lambda$ and compute the new equilibrium points.
3. Repeat steps 1 and 2 until λ is decreased by $\delta \lambda$ or until the maximum number of iterations n_{ite} is exceeded.

D. Saddle location control by local sensitivity analysis

Let x_0 be a stable equilibrium of model (8) with parameters π and let Assumption IV.1 hold. Let $s \in \mathbb{R}^n$ be a saddle point whose unstable manifold \mathcal{M}_s^u is heteroclinic to x_0 . Let $g_{s-x_0}(\pi) = \|s - x_0\|$ be the Euclidean distance between the saddle and the stable point as a function of the model parameters. By the chain rule $\frac{\partial g_{s-x_0}}{\partial \pi_i} = 2(s - x_0)^T \left(\frac{\partial s}{\partial \pi_i} - \frac{\partial x_0}{\partial \pi_i} \right)$, where $\frac{\partial s}{\partial \pi_i}$ and $\frac{\partial x_0}{\partial \pi_i}$ can be computed as in Lemma IV.1. It follows that the distance between s and x_0 is maximally increased along

$$d_{g_{s-x_0}} = \frac{\nabla g_{s-x_0}}{\|\nabla g_{s-x_0}\|} \quad (11)$$

where $\nabla g_{s-x_0} = \left[\frac{\partial g_{s-x_0}}{\partial \pi_1}, \dots, \frac{\partial g_{s-x_0}}{\partial \pi_m} \right]$. Given (11), we can formulate a control strategy to optimally increase $g_{s-x_0}(\pi)$ by $\delta g > 0$ units.

Control Strategy IV.2. Saddle Control

1. Compute (10) at the current equilibrium and parameter values.
2. Update the parameters: $\pi \leftarrow \pi + \varepsilon d_{g_{s-x_0}}$ and compute the new equilibrium points.
3. Repeat Steps 1 and 2 until $g_{s-x_0}(\pi)$ increased by δg or until the maximum number of iterations n_{ite} is reached.

E. Parameter sensitivity

The entries of the parameter control vectors d_λ and $d_{g_{s-x_0}}$, provide the sensitivity of the applied control to the parameters. Control is highly sensitive to parameters associated to entries with large absolute value: small variations of those parameters have large effects on the controlled quantity. Control is weakly sensitive to parameters associated to entries with small absolute value: big variations of those parameters are needed to affect the controlled quantity. In practice, highly sensitive parameters define the targets of experimental manipulations to bring a system to a desired state.

F. Multi-objective and underactuated control

There might be cases in which one needs to consider multiple control objectives at once, e.g., simultaneously increasing the distance between multiple equilibria, decreasing multiple eigenvalues, or any combination of the two control objectives. In such cases, new *multi-objective* control strategies based on Control Strategies IV.1 and IV.2 can be implemented using a Multiple-Gradient Descent Algorithm (MGDA) [9]. MGDA returns an optimal parameter control direction \tilde{d} by taking as input the gradients of the different control objectives and by returning a new gradient such that no objective is worsened. This method does not require additional hyper-parameters, e.g., the weights with which different gradients are weighted in the optimization procedure.

Another important case is when certain parameter manipulations are hard or impossible to achieve in practice, in which case we can introduce regularizing cost functions that penalize variations along those parameters or simply project those directions to zero before applying a gradient step. In this case, the resulting control strategy is called *underactuated*.

G. A Two-dimensional Monotone Example

Consider the following two-dimensional dynamics

$$\begin{aligned}\dot{x} &= -x^{n_x} + \alpha_x \tanh(x) - y + u_x \\ \dot{y} &= -y^{n_y} + \alpha_y \tanh(y) - x + u_y\end{aligned}\quad (12)$$

with $n_x, n_y \in \mathbb{N}$, $\alpha_x, \alpha_y, u_x, u_y \in \mathbb{R}$, which is a monotone (because two-dimensional and competitive [8, Example 1]) dynamical system with parameters $\pi = (\alpha_x, \alpha_y, u_x, u_y)$. Observe that the two exponents n_x, n_y are not controllable parameters and fixed to $n_x = 3$ and $n_y = 5$ in what follows.

Figure 4(a), shows the phase portrait of model (12) for nominal parameter values ($\pi = (3.0, 4.0, 0.3, 1.0)$). Our goal is to increase the basin of attraction of equilibrium e_6 (determined by the stable manifold branches highlighted in gray). We propose to do so by decreasing the real part of

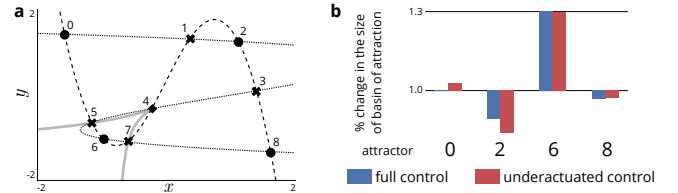


Fig. 4: Phase portrait of model (12) for nominal parameters (a). Stable steady-states are marked with circles, saddle points with crosses, and unstable points with diamonds. x -nullcline is dashed. y -nullcline is dotted. Saddle stable manifolds determining the boundaries of the basin of attraction of equilibrium e_6 are drawn in gray (b). Change in the size of the basins of attraction of the four stable equilibria e_0, e_2, e_6, e_8 under full (blue) and underactuated (red) control.

both eigenvalues λ_1, λ_2 of the linearization of model (12) at equilibrium 6 by at least 1.5 units each.² We apply Control Strategy IV.1 with MGDA [9] to simultaneously descend along the gradients associated to the two eigenvalues. The two control hyperparameters used are $\varepsilon = 10^{-2}$ and $n_{ite} = 1000$. As an illustration, in the underactuated control case only variations along the two most sensitive parameters were allowed, with the other two components projected to zero.

Figure 4(b) shows the result of our control strategy after 544 iterations. The size of the basin of attraction was estimated by randomly selecting initial conditions on the square $[-2, 2] \times [-2, 2]$ according to a uniform distribution and by recording the end state of each individual simulation. Simulation time was taken to be sufficiently long to ensure that practically steady-state was reached. The change in the size of the basin of attraction of each stable equilibrium e_0, e_2, e_6, e_8 was computed simply as the ratio between the number of initial conditions converging to it before and after control was applied. Both the full and the under-actuated control signal successfully increase the size of the basin of attraction of equilibrium e_6 by roughly 30%, while roughly maintaining or decreasing the size of the basin of attraction of the other stable equilibria.

V. CONTROL OF THE EMT REGULATORY NETWORK

Multistable networks like molecule and gene regulatory networks are described using a variety of *qualitative* modeling approaches, like boolean networks [10] and piece-wise linear models [11]. Data is indeed often unavailable to derive detailed quantitative models. The goal of qualitative models is mainly to capture binary molecular interactions and the transitions between different discrete cellular states. As suggested by [12], there is however a middle-ground between purely qualitative and detailed quantitative modeling, in which smooth ordinary differential equation (ODEs) models are not fitted to experimental data but, even so, variables and governing parameters remain quantitative. This allows a finer understanding of the model dynamics and, crucially, of the effects that variations of biologically relevant parameters have on them beyond all-or-none harsh manipulations like gene knock-in and knock-out.

²This choice is for purely illustrative purposes.

TABLE I: Four-dimensional reduction of the boolean model in [16] and associated boolean epithelial, senescent, and mesenchymal attractors. τ is the model discrete time. \neg denotes the boolean NOT operation. \wedge denotes the boolean AND operation. \vee denotes the boolean OR operation. .

$$\begin{aligned} S(\tau+1) &= \neg E(\tau) \vee (S(\tau) \wedge E(\tau) \wedge N(\tau)) \\ E(\tau+1) &= \neg S(\tau) \vee (S(\tau) \wedge E(\tau) \wedge \neg N(\tau)) \\ N(\tau+1) &= S(\tau) \vee E(\tau) \vee N(\tau) \vee P(\tau) \\ P(\tau+1) &= \neg S(\tau) \wedge ((E(\tau) \wedge N(\tau)) \vee P(\tau)) \end{aligned} \quad (13)$$

Gene (variable)	Epithelial	Senescent	Mesenchymal
<i>Snai2</i> (S)	0	0	1
<i>ESE2</i> (E)	1	1	0
<i>NFκB</i> (N)	1	1	1
<i>p16</i> (P)	0	1	0

A. Model derivation

Using boolean model reduction methods [13], [14], [15], it is possible to reduce the 9-dimensional boolean EMT model proposed in [16] to four boolean variables.³ This results in a system that evolves according to the boolean difference equation (13), which preserves key regulatory genes and all the attractors of the full model (Table I). Model (13) can be translated to a parameterized system of differential equations by mapping boolean operators to sum and products of increasing or decreasing sigmoidal functions. We use Hill functions $H(x, p, k) = \frac{x^p}{x^p + k^p}$ for increasing sigmoids and $\bar{H}(x, p, k) = 1 - H(x, p, k)$ for decreasing sigmoids. With these choices, we can map boolean operators to elementary algebraic operations between sigmoids:

$$\begin{aligned} \neg x &\mapsto \bar{H}(x, p, k), \quad x \wedge y \mapsto H(x, p_x, k_x) H(y, p_y, k_y) \\ x \vee y &\mapsto H(x, n_x, k_x) + H(y, n_y, k_y) \end{aligned}$$

Furthermore each interaction term is assumed to be parameterized by an interaction strength α , and each variable has a *linear degradation* term $-x$ and a constant *source term* β . The proposed translation from boolean to smooth ODEs is similar in spirit to [17] but with the crucial difference that interaction strengths and half-activations are parameterized, and that the smooth variables are not assumed to live in a unitary hypercube. The resulting quantitative dynamics are

$$\begin{aligned} \frac{dS}{dt} &= \alpha_1 \frac{k_1^p}{E^p + k_1^p} + \alpha_2 \frac{S^p}{S^p + k_2^p} \frac{E^p}{E^p + k_3^p} \frac{N^p}{N^p + k_4^p} + \beta_S - S \\ \frac{dE}{dt} &= \alpha_3 \frac{k_5^p}{S^p + k_5^p} + \alpha_4 \frac{E^p}{E^p + k_6^p} \frac{S^p}{S^p + k_7^p} \frac{k_8^p}{N^p + k_8^p} + \beta_E - E \\ \frac{dN}{dt} &= \alpha_5 \frac{S^p}{S^p + k_9^p} + \alpha_6 \frac{E^p}{E^p + k_{10}^p} + \alpha_7 \frac{N^p}{N^p + k_{11}^p} + \alpha_8 \frac{P^p}{P^p + k_{12}^p} \\ &\quad + \beta_N - N \\ \frac{dP}{dt} &= \alpha_9 \frac{k_{13}^p}{S^p + k_{13}^p} \left[\alpha_{10} \frac{E^p}{E^p + k_{14}^p} \frac{N^p}{N^p + k_{15}^p} + \alpha_{11} \frac{P^p}{P^p + k_{16}^p} \right] \\ &\quad + \beta_P - P \end{aligned} \quad (14)$$

Each lumped variable (S, E, N, P) is associated to a whole functional module of the actual EMT regulatory network. In the limit $p \rightarrow \infty$, Hill functions become binary activation functions and model (14) becomes piece-wise linear, as in [11].

³The reduction is not driven by computational limitations of the method, which can be scaled nicely to high dimensions using, e.g., automatic differentiation tools. However, reducing the model dimension reduces the number of parameters to be identified/tuned for the nominal EMT dynamical behavior while still providing qualitative insights into the processes to be manipulated in an experimental setting, as discussed below.

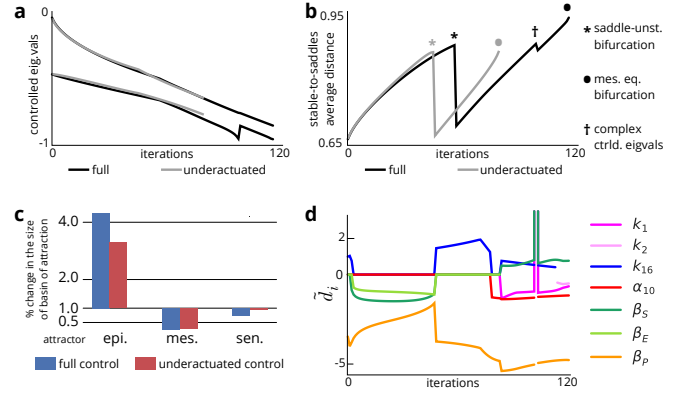


Fig. 5: **a.** Evolution of the two controlled eigenvalues across control iterations. **b.** Evolution of the average distance between x_e^* and saddle points delimiting its basin of attraction. **c.** Change in the size of the basin of attraction of the three stable equilibria after either the full control (blue) or the underactuated control (red) are applied. **d.** Components of the sensitive parameter control direction associated to the most sensitive parameters. \bullet : bifurcation of the mesenchymal stable equilibrium. $*$: bifurcation of one of the saddles delimiting the basin of attraction of x_e^* with another unstable equilibrium. \dagger : non-zero imaginary parts of the controlled eigenvalues.

B. Control through local sensitivity

For the nominal set of parameters π there are 3 stable points with purely real negative eigenvalues corresponding to the epithelial, senescent, and mesenchymal phenotypes, 3 saddle points separating their basins of attraction, and 1 unstable point. To verify that Assumption IV.1 holds for (14) with nominal parameters we numerically approximated the saddle unstable manifolds by picking initial conditions in a small neighborhood of each saddle and letting the trajectory converge. The resulting heteroclinic orbits were found to be monotone and revealed the presence of one saddle between the epithelial and senescent equilibria and of two saddles between the epithelial and mesenchymal equilibria. The epithelial and mesenchymal equilibria do not share boundaries of their basins of attraction. A Monte Carlo on initial conditions revealed that no other periodic or ‘strange’ attractors or separatrices existed. Finally, because the linear part of (14) is exponentially stable and the nonlinear part is bounded, it is easy to show that its trajectories are bounded and Assumption IV.1 holds.

Our goal is to increase the size of the basin of attraction of the epithelial equilibrium x_e^* . We do so by computing through MGDA the sensitive direction in the parameter space that simultaneously *i)* makes more negative the two eigenvalues of $J_{x_e^*}^\pi$ whose eigenvectors are tangent to the unstable manifolds of the saddle points surrounding x_e^* and *ii)* increase the average distance $\bar{g}_{x_e^* - s_{12}}$ between x_e^* and the two saddle points delimiting its basin of attraction. The stopping criterion is that all stable equilibria are maintained, i.e., none of them disappear in a bifurcation, or the maximum number of iterations $n_{\text{ite}} = 1000$ is reached.

The effects of the applied control strategy are summarized in Figure 5. Both controlled eigenvalues (Figure 5a) and $\bar{g}_{x_e^* - s_{123}}$ (Figure 5b) change in the desired direction across control iterations. As a consequence and as predicted by our theory,

the size of the basin of attraction⁴ of x_e^* is increased four-fold (Figure 5c), that of the senescent equilibrium shrinks slightly, and that of the mesenchymal equilibrium is reduced to approximately a third of its original size. The abrupt drops in the evolution of $\overline{g_{x_e^*-s_{12}}}$ correspond either to bifurcations of the model unstable equilibria or to some eigenvalues becoming complex at a stable equilibrium, which transiently violates Assumption IV.1 (see Figure 5 for details).

To test the robustness and practical applicability of our control strategy, we assumed that only three out of 32 parameters with the largest absolute sensitivity in \tilde{d} could be manipulated at each control iteration (while other components are projected to zero). This is again a kind of underactuated control. As summarized in Figures 5a,b,c, although a slight drop in performance can be detected, the control goal is robustly achieved.

Tracking the evolution of the components of the sensitive parameter control direction (Figures 5d) and, in particular, of the largest three used in the underactuated control strategy, reveals the key parameters to be manipulated and whether they should be increased or decreased. For instance, initially the three source terms (β_i , $i = S, E, P$) must all be decreased. Subsequently, the half-activation k_{16} must be increased and interaction gain α_{10} decreased. Due to model reduction, these parameters must be interpreted as lumped parameters corresponding to whole regulation pathways between four modules (associated to the lumped variables S, E, N, P) of the actual EMT regulatory network. The lumped parameter manipulations suggested by our method provide a qualitative guide of which molecular processes could be manipulated to achieve the same control objective experimentally.

VI. CONCLUSIONS

We derived a parameter control law to control the size and depth of the basins of attraction of multistable dynamics with simple attractors and simple separatrices. Monotone dynamical systems are important representatives of the class of models to which our method applies. Our control law is cheap to compute because it solely uses local, i.e., linearized, information of the model dynamics at its equilibria. When applied to biological models, our approach is able to suggest counter-intuitive parameter manipulations that can be tested in experimental settings to achieve desired control objectives. We illustrated this fact on the control of a new ODE model of the EMT, with relevance for the control of tumor formation and metastasis.

The main drawback of the proposed methodology is that it is grounded on a heuristic argument. It is therefore difficult to provide theoretical guarantees. For instance, the boundaries of the relevant basins of attraction might exhibit complicated shapes that are completely unpredictable by the local methods employed here. Despite enforcing both eigenvalues and saddle control, the boundaries of the basins of attraction might bend in such a way that the proposed control strategy would turn out disruptive for the control objective. An implicit claim

underlying this work is that *this cannot happen for monotone systems* but this still needs to be rigorously proved. Furthermore, beyond monotone dynamics, Assumption IV.1 must hold for our method to work. We were able to verify this assumption numerically for our EMT four-dimensional model but achieving the same in other models might not always be easy.

VII. CODE AVAILABILITY

The code used to run the paper simulations and generate the related figures, including the sets of used parameters, is available at GitHub: <https://github.com/rodrigo-moreno/basin-control-notebook>.

REFERENCES

- [1] A. N. Pisarchik and U. Feudel, "Control of multistability," *Physics Reports*, vol. 540, no. 4, pp. 167–218, 2014.
- [2] A. Bizyaeva, A. Franci, and E. L. Naomi, "Nonlinear opinion dynamics with tunable sensitivity," *To appear in IEEE Trans. Aut. Contr.*, 2022.
- [3] G. Balázsi, A. Van Oudenaarden, and J. J. Collins, "Cellular decision making and biological noise: from microbes to mammals," *Cell*, vol. 144, no. 6, pp. 910–925, 2011.
- [4] M. A. Nieto, R. Y.-J. Huang, R. A. Jackson, and J. P. Thiery, "EMT: 2016," *Cell*, vol. 166, no. 1, pp. 21–45, Jun. 2016, publisher: Elsevier. [Online]. Available: <https://doi.org/10.1016/j.cell.2016.06.028>
- [5] J. Yang and R. A. Weinberg, "Epithelial-Mesenchymal Transition: At the Crossroads of Development and Tumor Metastasis," *Developmental Cell*, vol. 14, no. 6, pp. 818–829, Jun. 2008, publisher: Elsevier. [Online]. Available: <https://doi.org/10.1016/j.devcel.2008.05.009>
- [6] R. Chakrabarti, J. Hwang, M. Andres Blanco, Y. Wei, M. Lukačičin, R.-A. Romano, K. Smalley, S. Liu, Q. Yang, T. Ibrahim, L. Mercatali, D. Amadori, B. G. Haffty, S. Sinha, and Y. Kang, "Elf5 inhibits the epithelial-mesenchymal transition in mammary gland development and breast cancer metastasis by transcriptionally repressing Snail2," *Nature Cell Biology*, vol. 14, no. 11, pp. 1212–1222, Nov. 2012. [Online]. Available: <https://doi.org/10.1038/ncb2607>
- [7] D. Efimov, "Global lyapunov analysis of multistable nonlinear systems," *SIAM Journal on Control and Optimization*, vol. 50, no. 5, pp. 3132–3154, 2012.
- [8] H. L. Smith, "Systems of ordinary differential equations which generate an order preserving flow. a survey of results," *SIAM review*, vol. 30, no. 1, pp. 87–113, 1988.
- [9] J.-A. Désidéri, "Multiple-gradient descent algorithm (MGDA) for multi-objective optimization," *Comptes Rendus Mathématique*, vol. 350, no. 5-6, pp. 313–318, 2012.
- [10] R. Somogyi and C. A. Sniegoski, "Modeling the complexity of genetic networks: understanding multigenic and pleiotropic regulation," *complexity*, vol. 1, no. 6, pp. 45–63, 1996.
- [11] H. De Jong, J.-L. Gouzé, C. Hernandez, M. Page, T. Sari, and J. Geiselmann, "Qualitative simulation of genetic regulatory networks using piecewise-linear models," *Bulletin of mathematical biology*, vol. 66, no. 2, pp. 301–340, 2004.
- [12] N. Le Novère, "Quantitative and logic modelling of molecular and gene networks," *Nature Reviews Genetics*, vol. 16, no. 3, pp. 146–158, 2015.
- [13] M. T. Matache and V. Matache, "Logical reduction of biological networks to their most determinative components," *Bulletin of mathematical biology*, vol. 78, no. 7, pp. 1520–1545, 2016.
- [14] A. Veliz-Cuba, "Reduction of Boolean network models," *Journal of theoretical biology*, vol. 289, pp. 167–172, 2011.
- [15] A. Saadatpour, R. Albert, and T. C. Reluga, "A reduction method for Boolean network models proven to conserve attractors," *SIAM Journal on Applied Dynamical Systems*, vol. 12, no. 4, pp. 1997–2011, 2013.
- [16] L. F. Méndez-López, J. Davila-Velderrain, E. Domínguez-Hüttinger, C. Enriquez-Olguín, J. C. Martínez-García, and E. R. Alvarez-Buylla, "Gene regulatory network underlying the immortalization of epithelial cells," *BMC systems biology*, vol. 11, no. 1, pp. 1–15, 2017.
- [17] L. Mendoza and I. Xenarios, "A method for the generation of standardized qualitative dynamical systems of regulatory networks," *Theoretical Biology and Medical Modelling*, vol. 3, no. 1, p. 13, 2006.

⁴Computed through a Monte Carlo on initial conditions in $[0, 4]^4$.